T. VUHERER, A. GODINA, Z. BURZIĆ, V. GLIHA

ISSN 0543-5846
METABK 46 (4) 237-243 (2007)
UDC - UDK 621.791.051:669.15=111

FATIGUE CRACK INITIATION FROM MICROSTRUCTURALLY SMALL VICKERS INDENTATIONS

Received - Primljeno: 2006-07-26
Accepted - Prihvaćeno: 2006-10-17
Original Scientific Paper - Izvorni znanstveni rad

The resistivity of a coarse grain steel against fatigue crack initiation in presence of micro-defects is discussed. Samples of material with martensitic microstructure were prepared by adequate thermal treatment. Microstructurally small Vickers indentations were used as artificial micro-defect. The compressive residual stresses are due to the irreversibility of plastic deformation. The moment of indenting enables to prepare samples with and without effects of residual stresses. The stress level for crack initiation depends on the actual indentation size. The location of initiated cracks is affected by the presence and character of residual stresses.

Key words: *micro-defect, coarse-grain heat-affected zone, crack initiation and growth, stress-concentration, fatigue limit*

Nastanak zamorne pukotine iz mikrostrukturno malih vickersovih otisaka. Proučavana je otpornost grubozrnatog dijela zone utjecaja topline na nastanak zamorne pukotine u prisustvu mikro greški. Uzorci materijala s martenzitnom grubozrnatom mikrostrukturom pripremljeni su odgovarajućom toplinskom obradom. Kao umjetne mikro greške upotrijebljene su mikrostrukturno mali Vickers otisci. Tlačna zaostala naprezanja pojave se zbog nepovratnosti plastične deformacije. Moment kad se napravi otisak omogućava pripremu uzoraka s i bez efekata zaostalih naprezanja. Kritička razina naprezanja za nastanak pukotine zavisi od stvarne veličine otiska. Na lokaciju nastanka pukotine utječe i prisutnost te vrsta zaostalih naprezanja.

Ključne riječi: *mikro greška, grubozrnata zona utjecaja topline, nastanak i rast pukotine, koncentracija naprezanja, zamorna čvrstoća*

INTRODUCTION

The welds consist of base material, heat affected zone (HAZ) and deposited metal. Figure 1. shows the schema of the weld microstructure. The filler material and part of the base material melt down during welding and form solidified weld metal, while, the base material in the close vicinity undergoes a transformation.

The HAZ formation is result of an applied thermal cycle caused by the heat source movement which is necessary to melt material. The effects of the thermal cycle diminish with the distance from the fusion line. The material close to the weld metal is heated almost to the melting point and the high temperature produces a grain growth. The result is the formation of a coarse-grained microstructure in the so-called coarse-grain heat-affected zone (CGHAZ) adjacent to the fusion line. This microstructure influences the mechanical properties, such as impact toughness and fatigue limit.

Due to the shape of solidified weld metal a concentration of the stress appears at the weld toes of loaded welds. The location of stress concentration in Figure 2. is marked as K_t (left, above). In order to avoid stress concentration, fine grinding of the weld reinforcement is sometimes performed, although it is economically hardly acceptable. If grinding is not carried out, the fatigue strength is certainly reduced.

Weld defects in the weld metal and HAZ appear mainly due to the insufficiently controlled process of welding. Non-destructive examination (NDE) methods are successfully used to ensure the soundness of welds. Defects that are smaller than the threshold sensitivity of the NDE method cannot be detected and the presence of those small defects in welds caused either by welding or base metal production can promote crack initiation during the cyclic loading. The final consequence of the defects is lower fatigue strength of welds.

The effect of defects on the fatigue limit of polycrystalline metals is negligible when the size of the defects becomes smaller than the biggest microstructural units [1]. Such microstructurally small defects are micro-defects.

T. Vuherer, A. Godina, V. Gliha, Faculty of Mechanical Engineering University of Maribor, Mabribor, Slovenia, Z. Burzić, VTI Beograd, Serbia

Grains are usually the biggest microstructural units of a CGHAZ.

During the cyclic loading at a sufficient stress amplitude fatigue cracks appear due to the interactive effect of micro-defects and applied stress. The first stage of the fatigue crack appearance is the crack initiation. In the presence of micro-defects of the size of microstructural units the crack initiation is easier because of the locally enhanced stress/strain field.

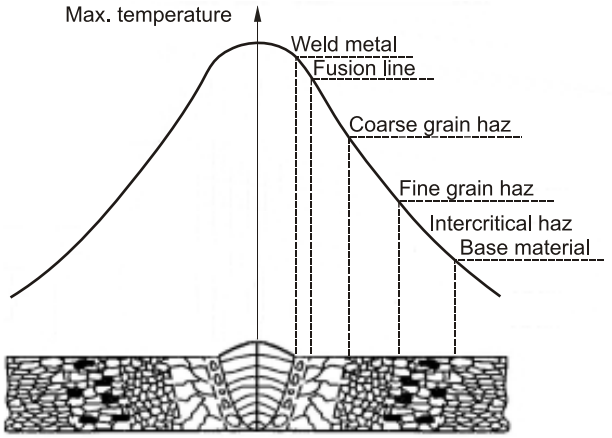

Figure 1. **The microstructure across the weld**
Slika 1. **Mikrostruktura u presjeku zavara**

The crack initiation from micro-defects is followed by fast crack growth [2]. In this early sequence of the fatigue crack propagation, the grain boundaries are strong barriers for crack growth.

However, the growth rate of cracks smaller than grains decreases when crack tip approaches to the grain boundary. If the level of cyclic stress is not sufficient to overcome such obstacles, crack growth will stop and the crack becomes a non-propagating.

Residual stresses present in welds in the as-welded condition [3]. Tensile residual stresses promote crack emanation from micro-defects, while compressive stresses have an opposite effect.

For the all above described reasons CGHAZ often represents the weakest link of cyclically loaded high quality welds because of:
- coarse grain microstructure,
- changed mechanical properties,
- welding residual stresses,
- stress concentration due to weld shape,
- presence of defects.

Only if fatigue tests are executed on actual welds and with in detail examination of specimens with initiated fatigue cracks the most critical HAZ microstructure can be located. The fatigue limit prediction of welds with or without micro-defects is therefore difficult.

The artificial HAZ microstructures can be used to study behaviour of different areas of welds during fatigue [4 - 8]. The advantages of this approach are:
- identical microstructure in an extensive volume of the sample,
- homogeneity of material, i.e. without present weld defects,
- absence of the welding residual stresses,
- possibility to simulate effects of defects by preparing the artificial micro-defects.

The fact that mechanical preparation of artificial micro-defects creates residual stresses is crucial for the behaviour of polycrystalline metals with such defects. The residual stresses can be of tensile or of compressive type and sometimes even of amplitude near to the yield point of the material. The main reason of residual stress appearance due to micro-defects preparation is the irreversibility of the material plastic deformation.

All residual stresses have effect on the fatigue crack initiation from micro-defects. Local very high residual stresses can even change the actual shape of the micro-defect.

To evaluate the effects of defect size to the fatigue limit alone, effects of residual stresses due to artificial defects preparation should be omitted. Electro-etching is usually used. Part of material with the highest stress is removed without any plastic deformation. In this way, the residual stress level is substantially lowered. Unfortunately, the removing of residual stresses with etching is accompanied with the change of shape and size of micro-defects.

The aim of this article is to discuss the influence of indenting residual stresses on the initiation of cracks from microstructurally small Vickers indentations in coarse grain steel.

MATERIAL AND EXPERIMENTAL PROCEDURE

Tests impossible to perform with samples from real welds, as the tensile, the impact test and the fatigue test etc, are easily to perform on specimens with an artificial HAZ microstructure prepared with simulation using either a weld thermal cycle simulator or a furnace.

Data on heating rate ($\dot{T}$), peak temperature (T_{max}) and cooling time ($\Delta t_{8/5}$) are used for the simulation of the thermal conditions during welding. The schema in Figure 2. (right, above) presents the temperature lapse during the preparation of CGHAZ microstructure using a weld thermal cycle simulator. The actual simulation is shown in the photograph (right, below). Few shapes of specimens with the limited volume of simulated CGHAZ microstructure located in the middle of the specimen's length (shaded areas) are shown in the drawing (left, below).

If CGHAZ microstructure is prepared in a furnace an appropriate heat treatment should be applied to the material

to obtain as coarse grain microstructure as relevant constituent. In the first part of the heat treatment a coarse grain annealing should be performed to obtain right grain size, in the second one, suitable quenching medium should be used to ensure the formation of the expected microstructural constituents. The main advantage of HAZ microstructure simulation in furnace is a homogeneous microstructure in the whole specimen not only in a limited volume.

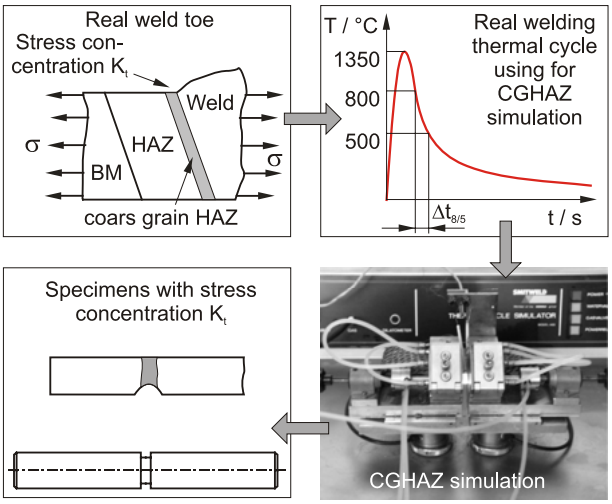

Figure 2. **The simulation of HAZ microstructure using a thermal-cycle simulator**
Slika 2. **Simulacija mikrostrukture ZUT upotrebom simulatora toplinskog ciklusa**

Nickel-molybdenum steel CT781 (W. Nr. 1.6587) with the chemical composition in Table 1. is used in this investigation.. The steel is used in the automotive industry.

Table 1. **Chemical composition of the steel CT781**
Tablica 1. **Kemijski sastav čelika CT781**

Elem.	C	Si	Mn	P	S
wt. / %	0,18	0,22	0,43	0,012	0,028
Elem.	Cr	Ni	Mo	Cu	Al
wt. / %	1,56	1,48	0,28	0,15	0,023

In order to form CGHAZ microstructure using weld thermal cycle simulator a thermal cycle with $\dot{T} = 200$ °C/s, $T_{max} = 1350$ °C, $\Delta t_{8/5} = 5$ s is applied to the steel. The simulation parameters define a "cold" welding producing a martensitic microstructure with the grain size of approx. 200 μm (Figure 3.a) and the hardness of 460 HV10.

The aim of CGHAZ microstructure simulation in furnace was to prepare the same microstructure in the whole sample (Figure 4.). At the first step suitably shaped samples of steel are heated to 1100 °C and held in the furnace for 3 hours. Grains grow to the size of approx. 200 μm. The coarse grain annealing is followed by cooling in water. The next step of the treatment is heating to 870 °C and water quenching. The result is a martensitic microstructure. The grain size and the hardness of this microstructure is the same as that prepared with the thermal cycle simulator; only the martensitic packets and plates are somewhat finer (Figure 3.b).

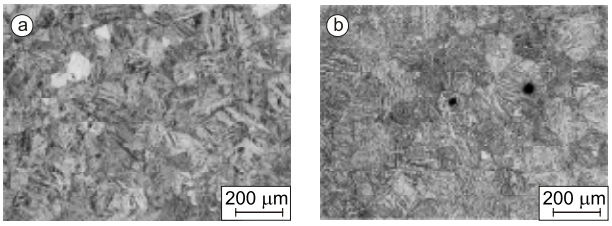

Figure 3. **Microstructure of the simulated CGHAZ: a) preparation using the welding thermal simulator, b) preparation in the furnace**
Slika 3. **Mikrostruktura simuliranog grubozrnatog ZUT: a) priprema upotrebom toplinskog simulatora zavarivanja, b) priprema u peći**

Rotary bending fatigue test was used to determine the fatigue limit of CGHAZ material. The dimensions of the circumferentially notched bend specimen are shown in Figure 5. The notch produces theoretical stress concentration factor of $K_t = 1{,}74$ [9]. Cyclic bend-loading produces an alternating stress with the rate of $R = -1$. The microstructurally small defects (micro-defects) at the bottom of the notch are prepared by indenting with a Vickers pyramid at the load 98,1 N. The diagonal of the indentations is of 200 μm, the depth is smaller because of the pyramid shape. It is obviously that the indentations are micro-defects because they are smaller than the biggest microstructural unit, i.e. average grain.

During the cyclic loading at a specified level fatigue cracks appear due to the interactive effect of the stress concentration due to the Vickers indentation and the applied stress. The crack initiation was detected, the test stopped and the specimen submitted to the examination in optical and scanning microscopes.

A relatively great volume of material is plastically deformed when indenting with a Vickers pyramid. The level of generated residual stresses depends on the material properties, their expansion in the volume of the deformed material. Unfortunately, electro-etching cannot be efficient to remove the effect of widespread residual stresses which is crucial for the fatigue crack initiation stage and the early growth of micro-cracks.

A new approach to remove residual stresses was necessary for the experimental work with indentations. The re-crystallisation during transformation in the last stage of CGHAZ furnace simulation seems a convenient way to remove the residual stresses without significant change of defect's geometry.

Therefore, two stress conditions of the specimen with Vickers indentations were prepared:

1. The as-indented condition, i.e. with residual stresses (indenting is executed after the complete heat treatment for CGHAZ simulation - point 2 in Figure 4.).
2. The residual stress-free condition, i.e. without residual stresses (indenting is executed before heating for water quenching - point 1 in Figure 4.).

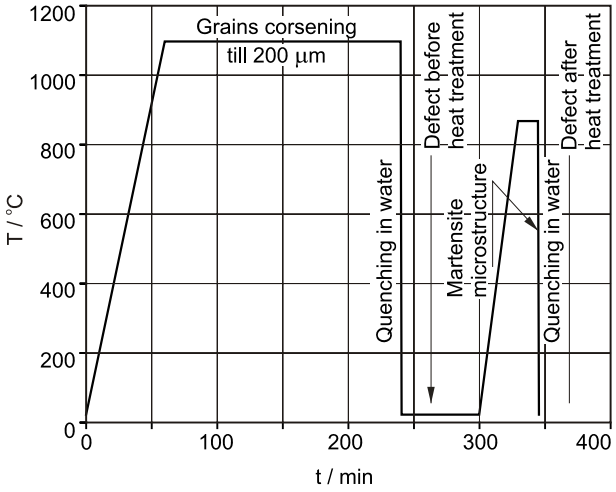

Figure 4. **The heat treatment for CGHAZ formation in the furnace**
Slika 4. **Toplinska obrada za oblikovanje grubozrnatog ZUT u peći**

RESULTS AND DISCUSSION

The combined effect of small defects, small cracks, small inclusions etc on the fatigue strength of metals was studied by Murakami and Endo more than twenty years ago [10]. They did not approach it as a notch problem. The fatigue limit of polycrystalline metals was interpreted as

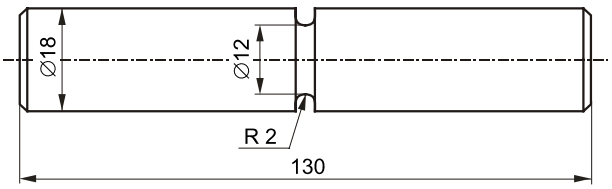

Figure 5. **Rotary bending specimen**
Slika 5. **Proba za rotaciono ugibanje**

the condition for non-propagation of cracks emanating from defects. They introduced a corresponding geometrical parameter of small defects with which the transition from the non-propagating crack to the propagating crack condition is defined.

Thus, the parameter $\sqrt{area}$ was proposed to evaluate influence of micro defect on the crack growth [10 - 12]. This parameter is the square root of an orthogonal projection of the micro-defect to the plane of applied stress and it was used with great success as quantitative measure for the detrimental effect of small defects on the fatigue strength of metals [13 - 18]. In fact, the greatest portion of published results is dealing with the effects of drilled small holes, though other kind of small defects were used, too. The geometrical concept of *area* of a Vickers indentation is shown in Figure 6. The first approximation is a triangle with baseline *d* (diagonal of indentation) and height *h* (depth of indentation).

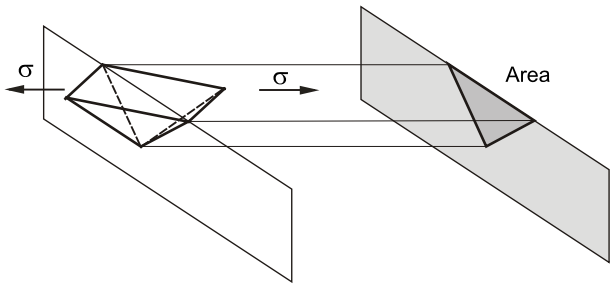

Figure 6. **Orthogonal projection of the Vickers indentation to the plane of applied stress**
Slika 6. **Ortogonalna projekcija Vickersovog otiska na ploštinu naprezanja**

If the diamond pyramid is assumed to be incompressible and the indented metal ideally plastic, value *area* of a Vickers indentation will be expressed by using the shape of Vickers pyramid and the measurable size of indentation on the surface. The angle between the opposite planes of Vickers pyramid is 136°. The angle, α, between the opposite edges that form the diagonal of the indentation, is above 136°. The depth h and angle α is calculated as:

$$h = \frac{d \cdot \sqrt{2}}{4} \cdot \text{ctg } 68°; \quad \alpha = 2 \text{ arctg} \left(\sqrt{2} \cdot \text{tg } 68° \right). \tag{1}$$

Unfortunately, the diamond pyramid is not incompressible, although its elastic modulus is at least 5 times higher than that of steels [19]. In addition, the residual stresses caused by indenting of strain-hardening elastic-plastic steel are compressive, since originating from the equilibrium of the applied indenting load (98,1 N) and the reaction of elastically deformed indented material. The indentation changes of shape after the load was removed when residual stresses arise. Therefore, the actual depths of indentations are smaller than the theoretically calculated using Eq. 1 [20, 21].

A special method schematically shown in Figure 7. was used for measuring of the actual profile of the Vickers indentation. The specimen is mounted on an accurate measuring table movable in one direction. The uncertainty of table position is 0,5 μm. Optical travelling microscope and laser interferometer are used for depth measurements. The microscope is used at the constant magnification of 1250. The diagonal of indentation is followed from the point where indentation appears to the point where indentation disappears. After the observed spot along the

diagonal is focused, microscope moves vertically and its former position is measured by a laser interferometer. The uncertainty of microscope position is 0,2 μm. By moving the table and microscope the whole profile of indentations is incrementally measured and data stored.

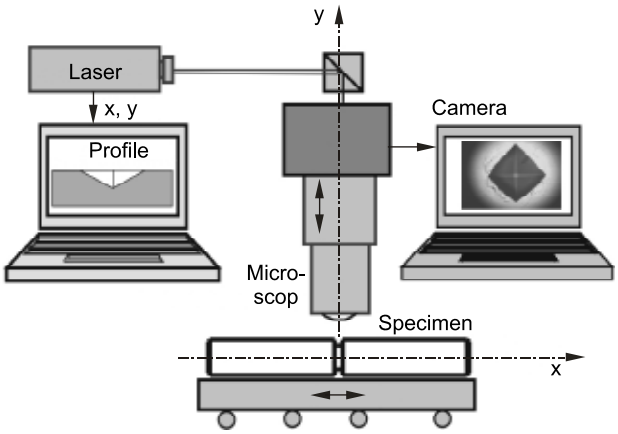

Figure 7. **Vickers indentation profile measurement**
Slika 7. **Mjerenje profila Vickersovog otiska**

Calculation and measurement were made with the same indentation. Its diagonal was 204 μm. The depth of the indentation calculated from Equation 1 is of 29,4 μm. The dashed line in Figure 8. represents the calculated profile. The calculated defect size parameter $\sqrt{area}$ is 55,1 μm.

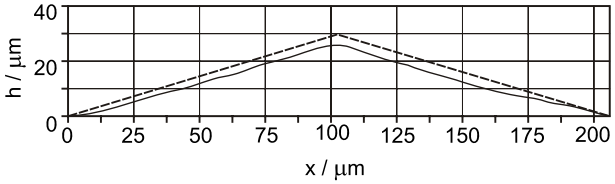

Figure 8. **Profile of the Vickers indentation (dashed line calculated from the shape of pyramid, solid line is measured)**
Slika 8. **Profil Vickersovog otiska (isprekidana linija line izračunata je iz oblika piramide, puna linija je izmjerena)**

The solid line in Figure 8. represents the measured profile. The actual depth of indentation is 26,0 μm. The calculated defect size parameter $\sqrt{area}$ is 50,5 μm, almost 10 % less than the theoretical value.

According to Murakami, the fatigue limit and threshold stress intensity factor of polycrystalline metals are calculated from parameter $\sqrt{area}$ and hardness [11, 12] as:

$$\sigma_w = \frac{1.43\,(HV + 120)}{\left(\sqrt{area}\right)^{\frac{1}{6}}},$$

$$\Delta K_{th} = 3{,}3 \cdot 10^{-3}\,(HV + 120) \cdot \left(\sqrt{area}\right)^{\frac{1}{3}}, \qquad (2)$$

where:

σ_w - the fatigue limit / MPa,
ΔK_{th} - the threshold stress intensity factor / MPa·m$^{1/2}$,
HV - the Vickers hardness number,
$\sqrt{area}$ - the defect's size parameter / μm.

The change of Vickers indentation size due to the produced residual stresses influences on the threshold stress intensity factor and the fatigue limit of material with the artificial micro-defect. The actual value of the defect size $\sqrt{area}$ decreased for 10 % causes increase the fatigue limit for 1,7% and decreases the threshold stress intensity factor for 3,3 %.

In the material treated as continuum, the surface cracks in a homogeneous stress field tend to the semi-elliptical shape with the height-to-length ratio (aspect ratio) approx. 0,4 [22]. Namely, the stress intensity factor range should be equal along the whole crack periphery.

The dimensions of Vickers indentation used as a micro-defect are length and depth, i.e. d and h (Equation 1). The stress intensity at the deepest point of the outlined ellipse is much higher than that at the surface. Therefore, the crack from Vickers indentation would initiate at the deepest point. Different crack grow rate due to different stress intensity range in different directions would gradually fulfil the necessary crack shape condition (aspect ratio approx. 0,4).

In the case of polycrystalline metals and micro-defects the stress intensity along the crack periphery cannot be defined. The stress/strain field depends on the orientation of grains, too. Nevertheless, the crack initiation at the deepest point of the used micro-defect is most likely.

Loading of the specimens during tests was constant. Striations on the fracture surface did not appear. However, the fracture surface patterns shown in Figure 9. enable to disclose the positions of crack origin. The existence of the radial ledges indicates the direction of crack growth. They can be traced back towards the crack origin.

In the sample of indented material shown in Figure 9.a the crack initiates at the deepest point of the indentation and grows in a convex semi-elliptic shape. This is schematically shown in the upper part of the figure. The arrows represent direction of the crack growth from the indentation outwards. This indented specimen was in the residual stress-free condition because indenting was performed before the final quenching (point 1 in Figure 4.).

The pattern of the fracture surface shown in Figure 9.b is telling different story. Two cracks initiate at the edges of indentation. Their growth and coalescence are schematically shown in the upper part of the figure. The direction of the cracks growth is represented by attached arrows. The crack front of already coalesced cracks is concave in the middle. During further growth the crack gradually changes to a convex semi-elliptic shape. This indented specimen was in the as-indented condition because indenting was performed after the final quenching (point 2 in Figure 4.).

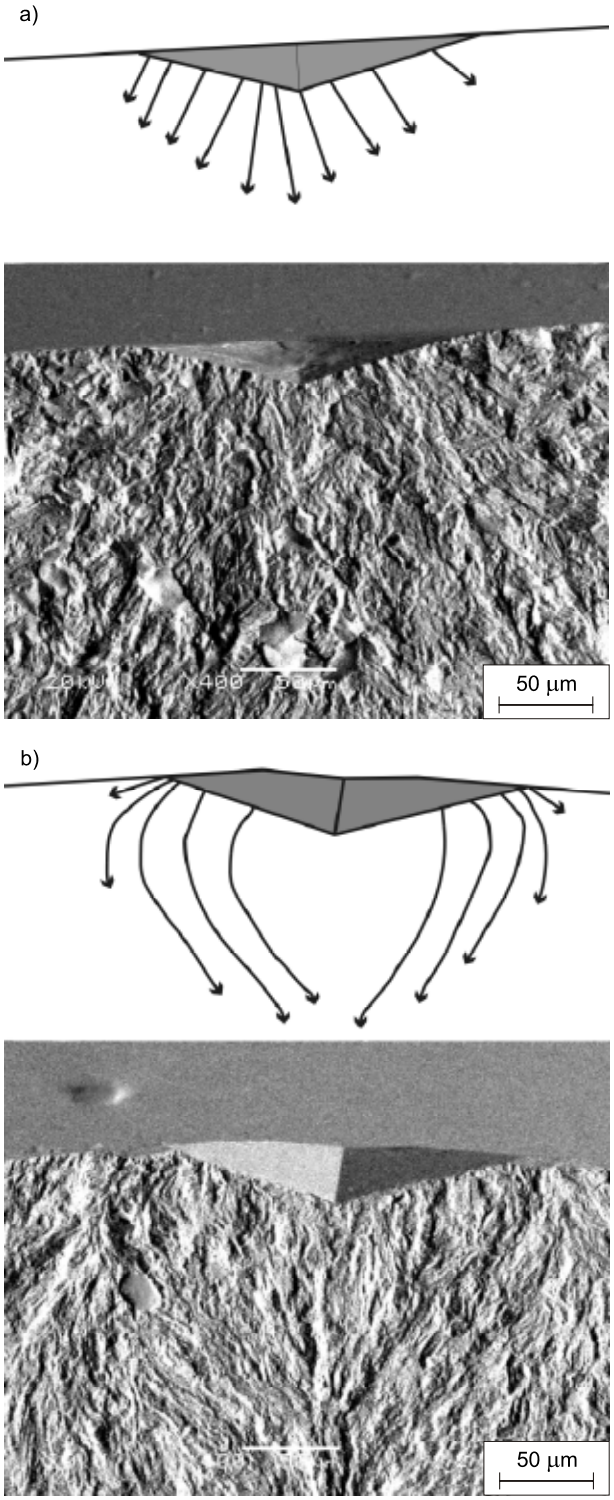

Figure 9. **Fracture surfaces of two indented specimens: a) residual stress free condition (crack origin is at the deepest point of the indentation), b) as-indented condition (cracks initiation is at the edges of the indentation)**

Slika 9. **Prelomna površina dvaju uzoraka sa otiskom a) stanje bez zaostalih naprezanja (pukotina nastala u najdubljoj točki), b) stanje sa zaostalim naprezanjima od otiskivanja (nastanak pukotine na rubovima)**

The reason for such unexpected crack behaviour during the initiation and early crack growth on indented specimen in the as-indented condition is a compressive residual indenting stress. This stress acts perpendicular to the edges of the indentation obstructing crack initiation. The magnitude of the compressive stress is the highest at the deepest point of the indentation. Crack initiation at both edges far away from the deepest point is easier because of lower compressive stress.

The correctness of the above described behaviour in the as-indented condition is proved in the microphotographs in Figure 10. of Vickers indentations in the bird's-eye view.

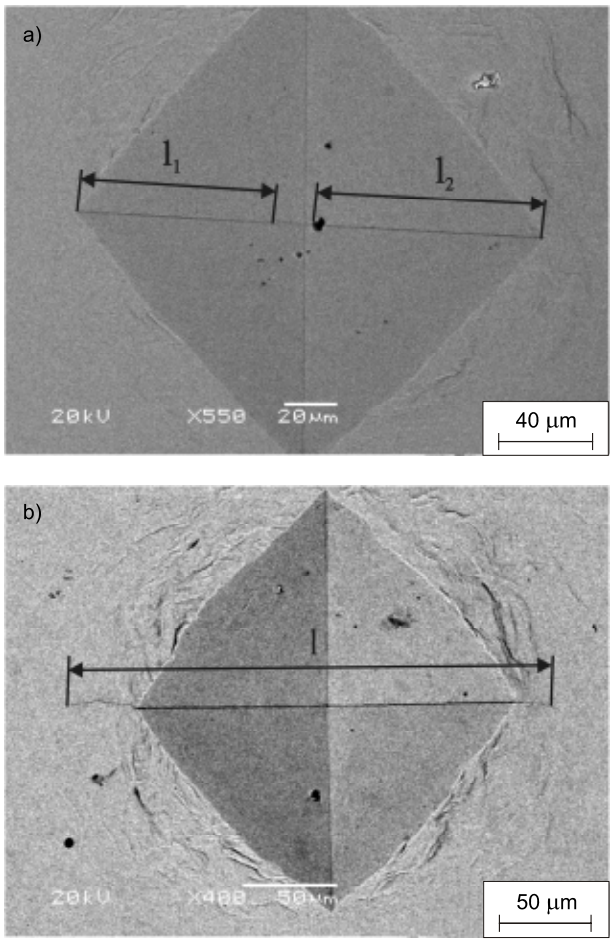

Figure 10. **Two stages of early crack growth on indented specimens in the as-indented condition: a) cracks developed at both edges, b) cracks are already coalesced and spread at the non-indented surface**

Slika 10. **Dva stupnja početnog rasta pukotina: a) pukotine se razvijaju na rubovima, b) pukotine su udružene i proširene na površinu**

In Figure 10.a two cracks were initiated a few tens of microns apart. In the moment of snap they are not jointed at the deepest point of the indentation. Their lengths are l_1 and l_2, respectively. They did not reach to the specimen's surface either. The next stage in the crack growth is shown

in Figure 10.b. The cracks are coalesced and already broke to the surface. The length of this non-propagating crack is l, more than sum total of l_1 and l_2.

Four stages of the life of indented specimens shown in Figure 11. schematically explain crack behaviour during the initiation and early growth in presence of residual stresses caused by indenting and their absence.

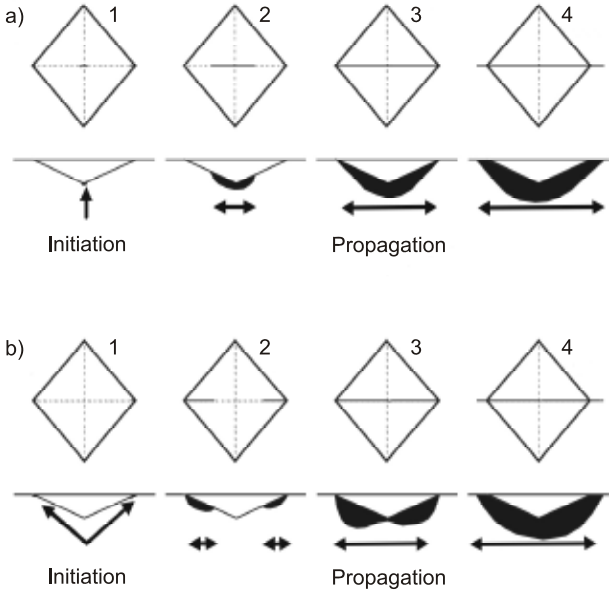

Figure 11. **Four stages of crack initiation and early growth from Vickers indentation: a) residual stress free condition, b) as-indented condition**

Slika 11. **Četiri stupnja nastanka i početnog rasta pukotine iz Vickersovog otiska: a) stanje bez zaostalih naprezanja, b) stanje s zaostalim naprezanjima od otiskivanja**

CONCLUSION

Indented notched specimens with the simulated microstructure of CGHAZ were fatigue tested. The crack initiation and its early growth was followed and analysed. The effects of residual stresses caused by indenting were discussed.

The actual shape of a Vickers indentation is needed to calculate the defect size parameter $\sqrt{area}$ which enables assessment of the fatigue limit, σ_w, and the threshold stress intensity factor, ΔK_{th}, of micro-defected materials. We found parameter $\sqrt{area}$ in the coarse grain steel used in this research almost 10% smaller than the expected one.

The residual stresses in the nearest surroundings of an artificial micro-defect have a decisive effect on the stress level necessary for the initiation of crack from a Vickers indentation. The presence of residual stresses, two cracks will initiate at both edges of the indentation. In absence of residual stresses, only one crack will initiate at the deepest point of the indentation.

REFERENCES

[1] H. Kitagawa, S. Takahashi, 2nd International Conference on the Behaviour of Materials, Boston 1976, p. 627 - 631.
[2] K. J. Miller, Fatigue and Fracture of Engineering Materials and Structures 10 (1987) 1, 75 - 91 and 93 - 113.
[3] T. Vuherer, Proceedings, Int. Conference MATEST '99, Croatian Soc. for Non - Destr. testing, V.Kstelj (ed.), Cavtat 1999, p. 95 - 102.
[4] V. Gliha, Proceedings, 12th Biennial Conference on Fracture - ECF 12, M. W. Brown (ed), E. R. de los Rios (ed.), K. J. Miller (ed.), Sheffield 1998, p. 193 - 198.
[5] V. Gliha, T. Vuherer, B. Ule, J. Vojvodič-Tuma, Science and Technology of Welding and Joining 9 (2004) 4, 399 - 406.
[6] T. Vuherer, V. Gliha, P. Yasniy, V. Hutsaylyuk, H. Nykyforchyn, Zavarivanje i zavarene konstrukcije 49 (2004) 3, 112 - 116.
[7] T. Vuherer, V. Gliha, V. Maver, P. Yasniy, H. Nykyforchyn, Proceedings, Dynamics, Strength and Reliability of Agricultural Machines, Nat. Acad. of Sci. Ukraine G.S Pysarenko Institute for problems of Strength, V. T. Troshchenko (ed), Ternopil 2004, p. 220 - 225.
[8] V. Gliha, Metalurgija 44 (2005) 1, 13 - 18.
[9] R. E. Petterson: Stress Concentration Factors; Charts and Relations Useful in Making Strength Calculations for Machine Parts and Structural Elements, John Wisley & Sons, New York, 1974, p. 27 - 31 and 69.
[10] Y. Murakami, M. Endo, Engineering Fracture Mechanics 17 (1983) 1, 1 - 15.
[11] Y. Murakami, M. Endo: The Behaviour of Short Cracks, xxx (ed.) vol.1, Mechanical Engineering Publication, London, 1986, p. 275 - 294.
[12] Y. Murakami: Effect of Hardness and Crack Geometries on ΔK_{th} of Small Crack Emanating from Small Defects, The Behaviour of Short Fatigue Cracks, K. J. Miller (ed.), E. R. de los Rios (ed.), Univer. Press Cambridge, 1986, p. 275 - 293.
[13] Y. Murakami, T. Nomoto, T. Ueda, Fatigue Fracture and Engineering Structure 22 (1999), 581 - 590.
[14] Y. Murakami, K. Matsuda: Small fatigue crack: Mechanisms and Applications Mechanics, (xxx ed.), Elsevier, 1999, p. 119 - 131.
[15] E. Endo: Effect of Small Defect on the Fatigue Strength of Steel and Ductile Iron Under Combined Axial/Torsion Loading, Small Fatigue Crack - Mechanics Mechanisms and Applications, K. S. Ravichandran (ed.), R. O. Ritchie (ed.), Y. Murakami (ed.), Elsevier, New York 1999, p. 375 - 387.
[16] M. Endo, I. Ishimoto, International Journal of Fatigue 28 (2006) 5-6, 592 - 597.
[17] V. Gliha, T. Vuherer, Proceedings, 3rd International Conference Fracture Mechanics of Materials and Structural Integrity, Nat. Acad. of Sci. Ukraine Karpenko Physico - Mech. Inst., V. V. Panasyuk (ed), Lviv 2004, p. 761 - 770.
[18] V. Gliha, T. Vuherer, Proceedings, 6th International Conference on Fatigue and Fracture - NT2F6, Brdo pri Kranju 2006, will be published.
[19] T. H. Courtney: Mechanical Behavior of Materials, McGraw-Hill, New York 1999, p. 59 - 60.
[20] Y. T. Cheng, C. M. Cheng, Surface and Coatings Technology 133 (2000), 417 - 424.
[21] Y. T. Cheng, C. M. Cheng, Philosophical Magazine Letters 78 (1998) 2, 115 - 120.
[22] Y. Murakami: Stress Intensity Factors Handbook, Vol. 1, Pergamon Press, Oxford, 1987, p. 42 - 45.